Ultraprecise Printing of *D*-Band Transmission Lines

Martin Roemhild, Georg Gramlich, *Graduate Student Member, IEEE*, Holger Baur, Thomas Zwick, *Fellow, IEEE*, and Norbert Fruehauf, *Member, IEEE*

***Abstract*— This letter discusses the fabrication of coplanar waveguide (CPW) transmission lines by ultraprecise deposition (UPD) and their characterization in the *D*-band (110–170 GHz). UPD is a direct printing process for the deposition of functional nanoinks. It has recently been introduced by XTPL as an alternative to aerosol jet and ink jet printing techniques. In UPD, a micrometer-scale nozzle is in direct contact with the substrate that is printed on. This approach allows the application of highly viscous nanoinks. A silver-filled ink with a viscosity exceeding 10^5 mPa·s is used in combination with a nozzle opening size of 5 μm to print CPWs with an air gap of 10 μm on Corning 1737 display glass and fused silica substrates. The lateral precision of the printing process is approximately 1–2 μm. To de-embed the transmission line performance, thru–reflect–line (TRL) calibration standards were manufactured on substrate. For a single, 400-nm-thick layer of the cured nanoink, the CPWs show approximately 1.0 dB/mm of loss at 140 GHz on fused silica and broadband transmission in the entire *D*-band.**

***Index Terms*— Additive manufacturing, aerosol jet printing, *D*-band, mmWave, radio frequency, ultraprecise deposition (UPD).**

I. Introduction

RF DEVICES have seen widespread use in recent years. Prospective applications, such as sensors for autonomous driving and industrial automation, and high data rate communication, demand large usable bandwidths. However, the frequency bands below 100 GHz are already widely used, and thus, the available bandwidth is limited. The *D*-band (110–170 GHz) is of interest, since it offers additional bandwidth and because chips in the *D*-band are still fabricable with contemporary silicon-based technologies. Complementing wafer-based semiconductor technologies, additive manufacturing has the potential to allow for highly modular designs of passive RF devices with precision that matches the back end of line of chip fabrication.

Ultraprecise deposition (UPD) is a promising candidate to achieve high-precision and low-cost printed passive devices, such as transmission lines. Feature sizes as low as 1 μm have been achieved with this approach [1]. This minimum feature size is significantly lower than what has been achieved with aerosol jet [2], [3] and ink jet printing [4] technologies. Previous work in UPD has dealt with single lines that were used for electrical connections at low frequencies of operation [1], [5], [6], [7], [8]. At radio frequencies, however, specialized transmission line geometries are required for low-loss, confined transmission of signals. In particular, coplanar waveguide (CPW) is attractive for a proof of concept, since it requires high precision along the entire length of the waveguide while being straightforward to de-embed. In this letter, we present UPD-printed conventional CPWs that are constructed by printing many single lines with well-defined spacing and shape on fused silica and Corning 1737 boro-aluminosilicate display glass substrates.

Manuscript received 29 June 2023; accepted 23 July 2023. Date of publication 11 August 2023; date of current version 9 October 2023. This work was supported by the Ministry of Science, Research, and the Arts of the State of Baden-Wuerttemberg, Germany, within the framework of the "Mobility of the Future" Innovation Campus (ICM). *(Corresponding author: Martin Roemhild.)*

Martin Roemhild, Holger Baur, and Norbert Fruehauf are with the Institute for Large Area Microelectronics (IGM), University of Stuttgart, 70569 Stuttgart, Germany (e-mail: martin.roemhild@igm.uni-stuttgart.de).

Georg Gramlich and Thomas Zwick are with the Institute of Radio Frequency Engineering and Electronics (IHE), Karlsruhe Institute of Technology, 76131 Karlsruhe, Germany.

Color versions of one or more figures in this letter are available at https://doi.org/10.1109/LMWT.2023.3300569.

Digital Object Identifier 10.1109/LMWT.2023.3300569

II. Printing Process

UPD is a printing process that works by depositing highly viscous inks through a nozzle that is in contact with the substrate. The non-Newtonian ink CL85, developed by XTPL, is used as the ink of choice in this work. The ink exhibits shear thinning [1], which reduces the viscosity when printing. The very high viscosity of more than 10^5 mPa·s of the ink enables the high precision of the printing process [1]. However, the non-Newtonian behavior has to be carefully considered when designing a printing pattern. This is particularly relevant at the beginning and end of each printed line. The built-in printing algorithm follows linear acceleration and deceleration of the nozzle and automatically reduces the pressure when deceleration starts. In contrast, for printing waveguides, it was necessary for us to implement a custom printing algorithm to decouple the point of pressure reduction from the point where deceleration starts to achieve a sufficiently homogeneous linewidth.

In an XTPL Delta printer, the nozzle is tilted at a certain tilt angle with regards to the substrate (see Fig. 1). This is done to ensure nozzle safety when moving the nozzle along the substrate during printing.

Printing polygons is done by overlap printing of multiple lines. In the coordinate system of our printer, the x-axis and the y-axis are parallel to the substrate, while the z-axis is perpendicular to the substrate. The rotational axis for the tilt is parallel to the x-axis. For our experiments, we used nozzles with 5-μm opening size, 8.5–9-bar printing pressure, 1.5-bar idle pressure, 50-μm/s printing speed, 25 μm/s^2 of acceleration and deceleration, and a tilt angle of 50°.

III. Design

This work deals with the performance of UPD-printed CPWs on fused silica and glass substrates in the *D*-band.

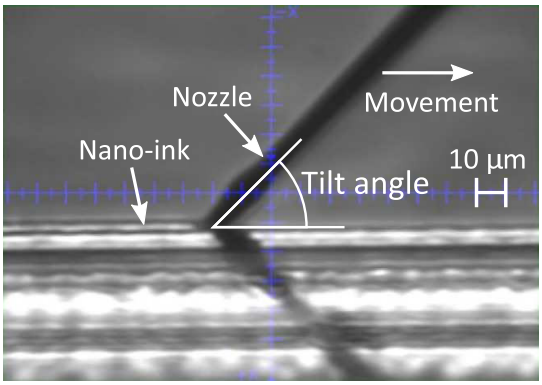

Fig. 1. Photograph of a nozzle with an inner diameter of 5 μm during printing.

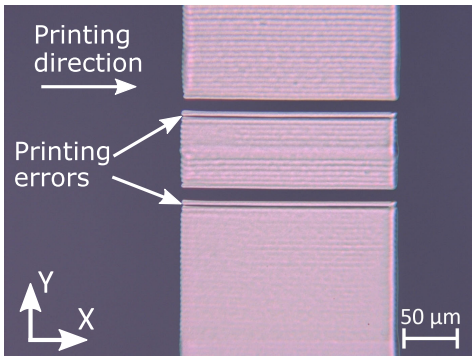

Fig. 2. Printing errors due to nozzle tilt in a reflect standard when printing in the X-direction.

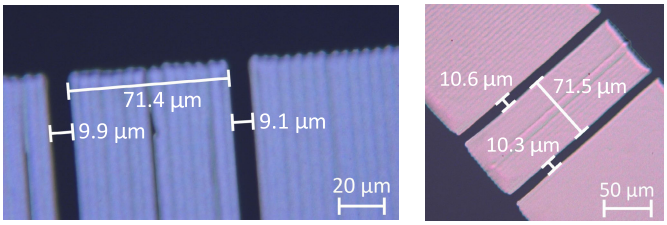

(a) (b)

Fig. 3. UPD-printed CPWs with a designed air gap of 10 μm, printed in (a) Y-direction and (b) 45°-direction.

The fused silica substrates have a thickness of 300 μm and the glass substrate a thickness of 1.1 mm. The substrates are prepared without any auxiliary layers for adhesion promotion, and the backside of the substrates is not metalized. This results in conventional CPWs without conductor backing. The CPWs are designed to be probeable with ground–signal–ground (GSG) probes for the D-band with a pitch of 100 μm. For this, the center conductor is designed to be 73-μm wide. With an air gap between center conductor and outer conductors of 10 μm, this results in a calculated characteristic impedance [9] of approximately 53 Ω on fused silica. Corning specifies the relative permittivity of the display glass as 5.7 at low frequencies. Assuming a similar ϵ_r in the D-band, this would result in a characteristic impedance of approximately 46 Ω for the same conductor dimensions as on fused silica. The dimensions were chosen as a compromise between the expected behavior during measurement of the two materials. The outer conductors are designed with a width of 150 μm each. For each substrate, the design includes three sets of calibration structures. Each set of calibration structures contains a thru with a length of 400 μm, an open with two 200-μm-long pads that are spaced 1 mm apart, and a line with 500-μm added length over the thru. In addition, there is also a second line that has 2.85-mm added length over the thru. This line is longer than the vacuum wavelength at 110 GHz. Hence, it will always be longer than a single wavelength in any material in the entire D-band. The long line is used to characterize the loss per length of the CPWs. To investigate potential influences of the nozzle tilt on the printing behavior, the aforementioned calibration structures and the 2.85-mm-long transmission line are included in the design in the y-direction, in the x-direction, and in a 45° angle between the x- and y-directions for each substrate.

IV. Fabrication

The process conditions are stabilized by fabricating in an ISO 5 cleanroom at constant temperature and humidity. Prior to printing, the substrates were blown with an ionizing blow-off gun. No further surface energy modifications were performed on the substrates before printing. The air gap is the most critical dimension of a CPW, particularly due to the risk of a short making the transmission line unusable. Even without a short, too high a variation in characteristic impedance would affect performance negatively. Because of this, the printed lines that flank the air gap are the most critical parts to fabricate. To reduce the risk of spillage near the air gaps, each of the lines directly next to an air gap was printed with a spacing of 5.5 μm to the succeeding line. All other lines were spaced by 5 μm. In addition, for each line flanking an air gap, the pressure is turned on later at the beginning and turned off further from the end of the line compared to the other lines. Decoupling the pressure turn-off point from the start of deceleration, as in our custom algorithm, proved crucial to ensure the same linewidth near the end of these lines. While these compromises lower the printed height in the vicinity of all air gaps, they are necessary to maintain the high precision where it matters. Conversely, spacing the printed lines too far apart leads to gaps in the conducting strips. In particular, when printing in x-direction, the nozzle tilt also needs to be considered to prevent gaps in the conductors. An example printing error due to an unconsidered nozzle tilt is shown in Fig. 2. These aberrations increase losses, which is discussed in Section VI.

Fig. 3 shows two fully UPD-printed CPWs with optimized parameters. The printed center conductor width and air gap in the pictures differ by less than 2 μm from the design. After printing, the ink is first dried in an oven at 120 °C for 10 min and then sintered, also in an oven, at 250 °C for 20 min. The ovens operate with air and are preheated. Between drying and sintering, the substrates are cooled to room temperature.

V. Measurement Setup

Thickness measurements were done with a Dektak 16 000 profilometer. The thickness measurements were taken perpendicular to the direction of signal propagation near the center of the 2.85-mm-long transmission lines. Surface roughness was measured with a Bruker Contour GT-K using white

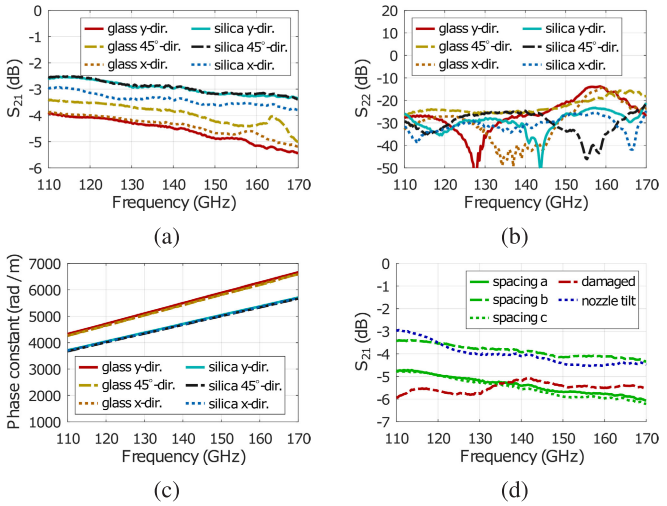

Fig. 4. Measured (a) S_{21}, (b) S_{22}, and (c) extracted phase constants of the 2.85-mm-long transmission lines on fused silica and glass substrates for different printing directions. (d) Measured S_{21} of example aberrations on fused silica substrates caused by too large spacing of printed lines in the conductor strips, damage during measurement, and nozzle tilt.

light interferometry. RF measurements were performed on a Keysight PNA-X with OML frequency extenders for the *D*-band. The used probes are Model 170 picoprobes by GGB. The calibration uses two tiers. The first tier is a line-reflect-reflect-match off-substrate calibration on a CS-15 impedance standard substrate. All on-substrate measurements were taken with this calibration. The second tier calibration uses the printed on-substrate thru–reflect–line (TRL) calibration structures to de-embed the measured results during postprocessing. Unless noted otherwise, the substrates were placed directly on a metalized chuck during measurement.

VI. Results and Discussion

Barring the presence of discontinuities, the most important aspect of a transmission line is the loss per length. The loss per length can be inferred from a measurement of S_{21} for a given length of the transmission line. Fig. 4(a) shows the measured S_{21} values for the 2.85-mm-long transmission lines on fused silica and glass substrates after applying the TRL calibration. Every shown measurement represents a line calibrated with its own TRL calibration structures.

All CPWs show transmission in the entire *D*-band. In Fig. 4(b), it can be seen that S_{22} remains below -21 dB for fused silica and below -13 dB for glass. The attenuation on fused silica at 140 GHz ranges from 2.95 to 3.4 dB, which corresponds to a loss per length of 1.0–1.2 dB/mm at this frequency. The losses on display glass were higher with a range of 1.4–1.6 dB/mm at 140 GHz. The phase constant $\beta = \omega\sqrt{\mu\epsilon}$ [10] can be used to extract $\epsilon_{\text{eff}} = (\epsilon/\epsilon_0)$. For the CPWs on fused silica [see Fig. 4(c)], an ϵ_{eff} of 2.51–2.57 can be extracted at 110 GHz. This increases to 2.53–2.57 at 170 GHz. For the CPWs on display glass, an ϵ_{eff} of 3.42–3.53 can be extracted at 110 GHz. This changes to 3.42–3.50 at 170 GHz. From this, characteristic impedances calculate [9] to approximately 53–54 Ω on fused silica and approximately 45 Ω on display glass, which is in good agreement with the expected behavior.

TABLE I
Comparison With Other Printed CPWs

Ref	Line loss in dB/mm	Feature size	t_{ink}	Technology
[2]	0.6 @ 170 GHz	$\geq 26\,\mu$m	$\approx 3.5\,\mu$m	Aerosol jet
[4]	0.5 @ 60 GHz	$\gg 10\,\mu$m	N/A	Ink jet
Here	1.0 @ 140 GHz	$\geq 10\,\mu$m	$\approx 0.4\,\mu$m	UPD

Fig. 4(b) shows the measurements of CPWs with gaps in the conductors due to too large spacing of the printed lines or nozzle tilt, and an example line where the porous ink was damaged by the probe tips during measurement. While the aberrations increase losses significantly when they appear, they can be reliably avoided by careful selection of process parameters and prudent measurement procedures.

For a single layer of ink, the printed thickness was approximately 400 nm. The printed thickness was lower when printed in the *x*-direction compared with the *y*-direction or 45°-direction. The surface roughness of the sintered ink is in the same order as the size of the nanoparticles. Approximate values for the surface roughness are an R_q of 51 nm and an R_a of 43 nm. This roughness is much lower than the best copper layers in Rogers RF-PCBs [11]. Hence, effects of roughness on losses and phase stability are expected to be negligible. Printing direction does not seem to affect roughness significantly.

Table I shows a comparison to different printing technologies. A value for t_{ink} was not given in [4]. Due to the lower thickness, the losses per length are higher in this work especially compared with [2], where five layers were printed. It should also be noted that UPD printing can take significant time. Printing slower or the lines closer together increases printed height, which would be a way to reduce losses. However, this would also further increase printing duration, and the additional material can reduce the printing accuracy, so it is not an option near critical parts of the structure. This aspect makes UPD currently more useful for printing smaller structures, which can be made more compact due to the lower minimum feature size of UPD.

VII. Conclusion

This work deals with UPD printing and characterization of CPWs for the *D*-band. The UPD printing process shows a lateral precision in the order of 1 μm. Such a high precision allows for the successful fabrication of CPWs with an air gap of 10 μm, exhibiting broadband performance in the entire *D*-band. The fabricated CPWs show losses of 1.0–1.2 dB/mm at 140 GHz on fused silica. These results exhibit the suitability of UPD as an alternative fabrication method for compact RF transmission lines above 100 GHz.

References

[1] M. Łysień et al., "High-resolution deposition of conductive and insulating materials at micrometer scale on complex substrates," *Sci. Rep.*, vol. 12, no. 1, Art. no. 9327, Jun. 2022, doi: 10.1038/s41598-022-13352-5.

[2] F. Cai, Y.-h. Chang, K. Wang, W. T. Khan, S. Pavlidis, and J. Papapolymerou, "High resolution aerosol jet printing of D-band printed transmission lines on flexible LCP substrate," in *IEEE MTT-S Int. Microw. Symp. Dig.*, Jun. 2014, pp. 1–3, doi: 10.1109/MWSYM.2014.6848597.

[3] G. Gramlich, R. Huber, U. Lemmer, and T. Zwick, "Aerosol jet printed millimeter wave interconnects in D-band," in *Proc. 52nd Eur. Microw. Conf. (EuMC)*, Sep. 2022, pp. 298–301, doi: 10.23919/EuMC54642.2022.9924311.

[4] B. K. Tehrani, R. A. Bahr, W. Su, B. S. Cook, and M. M. Tentzeris, "E-band characterization of 3D-printed dielectrics for fully-printed millimeter-wave wireless system packaging," in *IEEE MTT-S Int. Microw. Symp. Dig.*, Jun. 2017, pp. 1756–1759, doi: 10.1109/MWSYM.2017.8058985.

[5] A. Wiatrowska et al., "Ultraprecise deposition of micrometer-size conductive features for advanced packaging," in *Proc. IEEE 72nd Electron. Compon. Technol. Conf. (ECTC)*, May 2022, pp. 1573–1576, doi: 10.1109/ECTC51906.2022.00251.

[6] A. Wiatrowska et al., "59-3: Ultra-precise printing of micrometer-size interconnectors for high-resolution MicroLED displays," in *SID Symp. Dig. Tech. Papers*, vol. 52, May 2021, pp. 833–836, doi: 10.1002/sdtp.14812.

[7] S. Ma, Y. Kumaresan, A. S. Dahiya, and R. Dahiya, "Ultra-thin chips with printed interconnects on flexible foils," *Adv. Electron. Mater.*, vol. 8, no. 5, May 2022, Art. no. 2101029, doi: 10.1002/aelm.202101029.

[8] A. Wiatrowska et al., "Printing of micrometer-size features on complex substrates for system integration," in *Proc. IEEE 9th Electron. Syst.-Integr. Technol. Conf. (ESTC)*, Sep. 2022, pp. 273–276, doi: 10.1109/ESTC55720.2022.9939386.

[9] S. Gevorgian, L. J. P. Linner, and E. L. Kollberg, "CAD models for shielded multilayered CPW," *IEEE Trans. Microw. Theory Techn.*, vol. 43, no. 4, pp. 772–779, Apr. 1995, doi: 10.1109/22.375223.

[10] D. M. Pozar, *Microwave Engineering*, 4th ed. Hoboken, NJ, USA: Wiley, 2011, p. 98.

[11] Rogers Corporation. (2021). *Copper Foils for High Frequency Materials* Publication no. 92–243, Chandler, AZ, USA. Accessed: Jun. 23, 2023. [Online]. Available: https://www.rogerscorp.cn/-/media/project/rogerscorp/documents/advanced-electronics-solutions/english/properties—detailed-characteristics/copper-foils-for-high-frequency-circuit-materials.pdf